

# Sonoluminescing Gas Bubbles

I. Scott<sup>1</sup>, H.-Th. Elze<sup>1,2</sup>, T. Kodama<sup>2</sup> and J. Rafelski<sup>1</sup>

<sup>1</sup>Department of Physics, University of Arizona, Tucson, AZ 85721

and

<sup>2</sup>Universidade Federal do Rio de Janeiro, Instituto de Física  
Caixa Postal 68.528, 21945-970 Rio de Janeiro, RJ, Brazil

Revised August 1998

## Abstract

We draw attention to the fact that the popular but unproven hypothesis of shock-driven sonoluminescence is incompatible with the reported synchronicity of the single bubble sonoluminescence (SBSL) phenomenon. Moreover, it is not a necessary requirement, since we show that the sub-shock dynamic heating in gas bubble cavitation can lead to conditions required to generate intense 100ps light pulses. To wit we study the dynamics of the interior of a cavitating gas bubble subject to conditions suitable for sonoluminescence. We explore quantitatively the transfer of energy from the sound wave to the bubble interior, the frequency of atomic collisions in the bubble, the limits of quasi-stability of the non-linear bubble oscillations driven by an acoustical field, and obtain the implied reaction time scales.

PACS: 47.40.Dc, 47.10+g, 43.30.+m, 78.60.Mq

## 1. Introduction

Current interest in the gas bubble cavitation dynamics has been revived by the development of experimental conditions which allow a single bubble [1], trapped at the anti-node of a standing acoustic pressure wave, to emit relatively intense short light pulses [2]. This single bubble sonoluminescence (SBSL) displays considerable sensitivity to the experimental conditions and parameters. For a summary of the many ensuing experimental results we refer to the recent review by Barber *et al.* [3]. In particular they have found that the light flashes occur within 0.5 ns of maximum compression, last often less than 50 ps, comprise up to a million photons, and occur with synchronicity exceeding the frequency stability of the driving acoustical wave. The interplay of the diffusion processes and dynamical motion of the bubble has been also explored in depth [4] suggesting that there is ongoing diffusion of the gas between the bubble and the liquid, and that the gas contents of the SBSL bubble is result of self-fine-tuning dynamics (rectified diffusion).

The dynamics of the interior of the gas bubble and the energy inflow from the surrounding fluid into the bubble need to be understood in order to describe the energy focusing process in SBSL which is capable to convert acoustical energy into light. For sub-shock, spherical bubble dynamics we develop here a modification of the original Rayleigh-Plesset (RP) cavitation model [5], which

addressed only the dynamics of the spherical gas-liquid interface. The bubble interior enters the RP-model in terms of the (average) bubble gas pressure contributing to the surface dynamics and relevant in particular in the collapse phase. Our extension, based on variational approximation of hydrodynamics [6, 7], accounts also for the kinetic energy of the gas in the bubble. In this approach we develop further the observation made earlier regarding the homologous bubble shape [8], but we allow for an adiabatic change of the bubble density function between the collapse and expansion phases. Our sole present objective is to establish that there is rapid transfer of energy in sufficient quantity to the bubble, and that the bubble energy quenching occurs equally rapidly on sub-nanosecond scale. In this way we show that the required energy focusing can be accomplished just in a short time interval without inception of shock waves in the bubble, and that it arises from a combination of highly non-linear bubble dynamics and rapid quenching by acoustical radiation of bubble energy content [9].

Following a general discussion of the shock wave mechanism in the SBSL phenomenon in section 2, we develop in section 3 the variational hydrodynamic description of the gas in the interior of the bubble. In section 4 we present numerical solutions and we study the dynamics of the energy flow to the gas bubble, and explore the dynamics of matter and energy within the bubble. We summarize our results in section 5.

## 2. Shock waves and light pulses in SBSL

Perhaps the most popular proposed SBSL explanation up to this day involves the hypothesis that in order to generate the ultra-short 50ps light pulses seen in SBSL [3, 10] one has to resort to extreme conditions that require shock wave formation in the bubble. Numerical hydrodynamic flow models incorporating inward shock formation [11, 12], as well as possibly outward motion shocks [13] have been studied. Despite considerable effort it is hard to prove convincingly that shock waves are the power-source behind SBSL [14]. This is so, since there is no clear understanding how the shock motion energy is converted into light pulses that depend very sensitively on the atomic composition of the bubble. The only reason we see for shock mechanism popularity is that the extreme matter conditions associated here with SBSL naturally last for a relatively short time period, well within the lifespan of the SBSL light pulse, which were originally reported to be less than 50ps long [3]. More recently, depending on the details of the SBSL conditions, pulse-length in excess of 100ps has been reported [10].

Since we can obtain such time scale in section 4 without shocks, one must ask if the shock hypothesis should not be abandoned, for there is a serious internal inconsistency: only perfectly spherical inward shock could be reflected without destroying the bubble. However, light emission asymmetry has now been observed [15]: there is a class of SBSL events in which significant light ellipticity in the bubble is required, at the level of 20%. It is natural to associate this asymmetry with matter distribution asymmetry. But then an inward shock wave could not bounce, the bubble matter would spray outwards, the bubble would burst. Even if a bubble were to be rapidly (i.e. within a cycle of the driving harmonic pressure field) recreated, there remains a contradiction with the well advertised magic of SBSL, that synchronous light pulses are emitted over billions of shock cycles with timing precision exceeding significantly that of the driving acoustical field generator. We recall that for this reason SBSL has even been proposed as a possible cheap and precise clock [16].

Should we accept as argued that inbound shocks destroy the bubble, they will also erase bubble ‘memory’. The enhancement of temporal precision of cycle definition would have to arise from the liquid alone, a highly improbable situation, for which a mechanism is not in sight. An outward shock would not need to be reflected, but then the light pulse would be produced at the interface between gas and liquid, which is also inconsistent with the experimental results [15]. In our opinion

the precision of light pulse periodicity can only arise from nonlinear dynamics within the gas bubble to which the external pressure field in the liquid is merely an energy source and hence it can be oscillating at a less well determined frequency.

But what mechanism can produce light, if there is no shock? It is natural to expect that the light emitted is product of dynamical processes in the bubble. Any microscopic light production mechanism which does not generate strong spectral lines is suitable, including radiation from neutral atom collisions with continuum emissions[17]. This collision induced emission (CIE) mechanism for generation of SBSL-light pulses appears most consistent with the reaction framework we are proposing here. CIE process relies on relatively frequent and sufficiently energetic atomic collisions in high density matter. To address qualitatively the viability of this mechanism, we establish below in more detail the frequency of two-body atomic collisions at relative atomic energy that would allow the light pulse formation. While we do not pursue further more involved atomic physics aspects of the CIE process, we note that the densities reached in the bubble at sonoluminescence implicate three and more body collisions.

We note that a bubble with radius similar to light wavelength is not opaque to radiation, which thus is not emitted from a surface. Light emitted from the bubble center will not show features characteristic of being in equilibrium with the (thermal) source. Therefore the conclusion that thermal radiation is excluded [18], is not at all providing evidence for shock-waves as the mechanism of SBSL.

Another non-shock process has been proposed as mechanism for SBSL, involving strong, jet-like deformations invoked by the translational motion of the bubble in the gradient of the acoustical field [19]. While jets indeed are likely to develop as the bubble begins to collapse, in our opinion the long term bubble stability implies here that the increasing internal bubble density and the increasing surface tension are capable to stabilize the spherical shape of the bubble preceding the short final collapse phase, during which the SBSL light is emitted [20]. Were this not the case, the jet would have to excite SBSL in the final stages of bubble collapse with a non-negligible chance for bubble destruction.

### 3. Variational bubble hydrodynamics

Our theoretical extension of the standard RP approach concerns the dynamics of an ‘adiabatically’ homologous gas flow. This means that the shape and velocity of the interior matter are governed by the rapidly evolving radius parameter  $R(t)$  and surface velocity  $\dot{R}(t)$ , allowing for slower change in the homologous shape of matter characterized by a collective shape parameter  $a(t)$ . In order to exploit this to the fullest, we implement the dynamics within the variational hydrodynamical method [7], which has been discovered nearly 40 years ago (see Ref. [6], section 13, and references therein). Using the variational approach we sidestep the need for a full hydrodynamic solution of the gas motion. This simplified approach is suitable only for exactly spherical, (quasi) one-dimensional motion, and corresponds to a variational solution of the hydrodynamic problem with irrotational flow.

We consider a gas bubble of radius  $R(t)$ , shape  $g(x, a(t))$  mass  $M_G = \frac{4}{3}\pi R_0^3 \rho_0$  (expressed in terms of the initial radius  $R_0$  and density  $\rho_0$ ) surrounded by an incompressible liquid of density  $\rho_L$ . In terms of the  $R$ -scaled radial variable, the mass-conservation constraint,  $\dot{M}_G = 0$ , implies:

$$\rho_G = \frac{M_G}{4\pi R(t)^3} g(x, a(t)), \quad x = \frac{r}{R(t)} < 1, \quad (1)$$

$$\int_0^1 x^2 g dx = 1, \quad \int_0^1 x^2 \frac{\partial g}{\partial a} dx = 0. \quad (2)$$

$R(t)$  and the collective variable  $a(t)$  are the dynamical functions we will consider.  $a(t)$  comprises two important physical phenomena:

1. the slow underlying variation ('drift') describes how the shape of the mass density in the bubble changes between the contraction and expansion phases of the bubble motion – solving at fixed  $a = \text{Const}$ . We are implying that the shape shift is adiabatic compared to the rapid matter flow, expressed by changes in  $R$ ;
2. small, but rapid oscillation of  $a(t)$  may be superposed with this slow drift; they correspond to the acoustical cross-talk oscillations between the surface and the interior of the bubble with frequency  $\omega \simeq c_s/R \leq 10^9 \text{s}^{-1}$ , where  $c_s$  is the sound velocity in the gas.

The introduction of  $a(t)$  rather than time  $t$  in definition of the shape function  $g$  in Eq. (1) serves to separate these two types of non-homologous dynamics of the bubble.

In order to determine the dynamics of the gas bubble, we will seek an extremum of the action for the combined gas-liquid system using as dynamical variables  $R(t)$ ,  $\dot{R}(t)$ ,  $\dot{a}(t)$ ,  $a(t)$ . The matter shape function  $g(x, a)$  is imposed by the external constraints. The kinetic energy of the gas can be easily expressed as a function of  $g$ : solving the continuity equation we obtain the local flow velocity in the gas bubble:

$$v(r) = x\dot{R} - R\dot{a}\delta, \quad \delta = \frac{1}{x^2 g(x; a)} \int_0^x dx' x'^2 \frac{\partial g}{\partial a} \xrightarrow{x \rightarrow 1} 0 \quad . \quad (3)$$

After some integrations by parts of the time integral (action) the contribution in action is found [7]:

$$K_G = \frac{M_G}{2} \left\{ -I_1 R \ddot{R} + I_3 \dot{a}^2 R^2 \right\}, \quad (4)$$

with:

$$I_1 = \int_0^1 dx x^4 g, \quad I_3 = \int_0^1 dx x^2 g \delta^2. \quad (5)$$

When  $\delta$  is neglected ( $\frac{\partial g}{\partial a} \rightarrow 0$ ) one is in the exact homologous limit.

Eq. (4) complements the kinetic energy of the incompressible liquid of density  $\rho_L$ . Solving the continuity equation we obtain the local flow velocity and thus also the kinetic energy in the liquid:

$$v_L = \dot{R} \frac{R^2}{r^2}, \quad r > R; \quad K_L = 4\pi \rho_L R^3 \frac{\dot{R}^2}{2}. \quad (6)$$

The internal (potential) energy of the gas is:

$$W_G = W_G[R, g(x; a)] = \int \varepsilon(r, t) d^3r = M_G \int_0^1 dx x^2 g \mathcal{E}, \quad (7)$$

where  $\varepsilon$  is the energy density and

$$\mathcal{E} \equiv E/N = \varepsilon/\rho$$

is the specific energy of the gas. The total potential energy  $W$  of the bubble (normalized to zero for a bubble at rest under ambient conditions (pressure  $P = P_0$  and temperature  $T = T_0$ )) is:

$$W = W_G + 4\pi\sigma(R^2 - R_0^2) - P_L(V_0 - V_G). \quad (8)$$

We note that the second term in Eq. (8) is the energy from the fluid-gas interface, and  $P_L = P_0 + P_a(t)$  is the pressure in the liquid arising from the atmospheric pressure and any further time dependent externally applied (acoustical) pressure. Setting  $I_1 = I_3 = 0 = K_G$  i.e. ignoring

the interior dynamics of the bubble, and varying  $K_L - W$  with respect to  $R(t)$  one obtains the (improved) RP-model equations [21].

We first determine the dynamical equations which characterize the drift in  $a(t)$ . The tool of convenience here is the Hamiltonian for the motion of this dynamical variable. The generalized momentum following from Eq. (4) is:

$$\Pi_a = \frac{dK_G}{d\dot{a}} = \dot{a}I_3(a)R^2M_G, \quad (9)$$

and the Hamiltonian for the gas is then

$$\mathcal{H}_G(a, \Pi_a) = \frac{1}{2} \frac{\Pi_a^2}{\mathcal{M}_a} + \mathcal{V}_a. \quad (10)$$

Where the (collective) mass  $\mathcal{M}_a$  and potential  $\mathcal{V}_a$  are:

$$\mathcal{M}_a \equiv I_3(a)R^2M_G, \quad \mathcal{V}_a \equiv \frac{M_G}{2}I_1(a)R\ddot{R} + M_G \int_0^1 dx x^2 g(a)\mathcal{E}[\rho(a)]. \quad (11)$$

where  $I_1, I_3$  are given in Eq. (5). The rapid oscillations inherent in the harmonic Hamiltonian presented are centered around the minimum of  $\mathcal{V}_a$ , which drifts as the values of  $R, \ddot{R}$  change. At the same time there is a drift in the mass  $\mathcal{M}_a$  which impacts the frequency of the rapid oscillations, but not the location of the minimum of  $\mathcal{V}_a$ . thus if we study solely the drift in  $a$ -coordinate, we are effectively neglecting the deviations from the homologous shape inherent in the  $\delta$ -dependence of  $I_3$ .

As we search for the minimum of the effective potential in order to derive equations governing this motion we will need to invoke a few simple thermodynamic properties. From the first law of thermodynamics we recall the relation of pressure  $P$  to the internal specific energy  $\mathcal{E}$ :

$$P = - \left( \frac{\partial E}{\partial V} \right)_{|S,N} = \rho^2 \left( \frac{\partial \mathcal{E}}{\partial \rho} \right)_{|S}. \quad (12)$$

The heat function (enthalpy)  $h$  is introduced in view of the relation:

$$\frac{d}{d\rho} \left( \mathcal{E} + \frac{P}{\rho} \right)_{|S} = \frac{1}{\rho} \frac{dP}{d\rho} \Big|_S \quad \longrightarrow \quad h \equiv \mathcal{E} + \frac{P}{\rho} = \int_{S=Const} \frac{dP}{\rho}. \quad (13)$$

The minimum of  $\mathcal{V}_a$  determines the drifting value of  $a$ , which is obtained by solving:

$$\frac{1}{M_G} \frac{d\mathcal{V}_a}{da} = \int_0^1 dx x^2 \frac{\partial g}{\partial a} \left\{ h[\rho] - h_c + \frac{1}{2} x^2 R \ddot{R} \right\} = 0. \quad (14)$$

Here we have introduced a constant  $h_c$ , which integrates to zero by the second expression in Eq. (2), and which assures that the solution of Eq. (14) is found where the curly bracket in Eq. (14) vanishes. Considering the limit  $x^2 \rightarrow 0$  we see that  $h_c = h(x=0)$ . Differentiating with respect to  $x^2$  the argument of the curly bracket we obtain, under adiabatic constraints and using the definition of  $h$ , see Eq. (13):

$$-\frac{1}{2} R \ddot{R} = \frac{d}{dx^2} \{ h[\rho] - h_c \} = \frac{\partial \rho}{\partial x^2} \frac{\partial P}{\partial \rho} \frac{\partial h}{\partial P}, \quad (15)$$

and thus:

$$\frac{\partial}{\partial x^2} \ln g(x; a) = - \frac{R \ddot{R}}{2c_s^2(\rho(g))}, \quad c_s^2(\rho) = \frac{\partial P}{\partial \rho}, \quad (16)$$

where  $c_s$  is the local sound velocity in the gas. Here the factor  $R\ddot{R}$  is to be seen as a given parameter; in reality it is determined by the usual RP-dynamics, which does not depend much on the inclusion in the dynamics of the bubble interior kinetic energy of the. Thus Eq. (16) can be solved independently of the RP-dynamics, yielding the interior shape of the bubble at each phase of the dynamical evolution of bubble radius. We note that the sign of the RP-force factor  $R\ddot{R}$  in Eq. (16) determines the gradient of the density shape function: when the bubble is collapsing, the surface density is higher than the interior density, while when it is expanding the opposite is the case, and a flat distribution is found in the force free instants of the bubble motion, when  $\dot{R} = 0$ . We have explored elsewhere other theoretical features not discussed in depth here, such as the small fluctuations in  $a(t)$  [7], the back-reaction of the bubble dynamics into the RP-equations [7], non-perturbative treatment of the sound emission[9]. Also, we have obtained Eq. (16) for  $g(x, a)$  directly from the Euler equation in the limit  $\delta \rightarrow 0$ .

We note that only for a particular choice of the initial condition  $g(x=0)$  can we obtain a properly normalized solution of the nonlinear differential equation, Eq. (16). However, this we can do easily for any EOS subject to an adiabatic constraint, and specifically also for the van der Waals system we consider here, with finite size correction to the volume in the polytropic equation of state:

$$P[\rho] = P_0 \left( \frac{\rho_m}{\rho_0} - 1 \right)^\gamma \left( \frac{\rho}{\rho_m - \rho} \right)^\gamma, \quad h[\rho] = \frac{1}{\gamma - 1} \frac{P}{\rho} \left[ \gamma - \frac{\rho}{\rho_m} \right], \quad \mathcal{E}[\rho] = \frac{P}{\gamma - 1} \left( \frac{1}{\rho} - \frac{1}{\rho_m} \right), \quad (17)$$

with  $\rho_m \equiv M_G/a^3 = 3M_G/4\pi r_m^3$  and  $r_m$  is the van der Waals excluded radius.

#### 4. Physical properties of sonoluminescing bubbles

The motion of the bubble is primarily damped by sound radiation in the crash phase. We have determined that in rough detail a full treatment of the sound radiation is equivalent to first order in  $\dot{R}/c$  description when adjustment (i.e. fit) of the damping constants is allowed for [9]. We thus follow the approach of Löfstedt [21] and account for the sound damping influence on dynamics of  $R(t)$  by including the appropriate first order in  $\dot{R}/c$  terms in our extended Rayleigh-Plesset equation. We also incorporate the damping due to liquid viscosity. We do not study the effect of compressibility of the fluid surrounding the gas bubble. We use the parameters adjusted in Ref. [21] to fit the dynamics of the bubble radius.

The standard example we consider here is an argon gas bubble comprising  $N_G = 10^{10}$  atoms immersed in water. The parameters of the liquid are: density  $\rho_L = 1 \text{ g/cc}$ , surface tension  $\sigma = 0.03 \text{ kg/s}^2$ , sound velocity  $c_{H_2O} = 1450 \text{ m/s}$ , and viscosity  $\eta = 3 \cdot 10^{-3} \text{ kg/(ms)}$ . The equilibrium radius of a bubble under ambient pressure  $P_0 = 1 \text{ atm}$  at ambient temperature  $T_0 = 277K$  obtained from the van der Waals equation state is  $R_0 = 4.39 \mu\text{m}$  and the excluded radius parameter is  $a = 0.503 \mu\text{m}$ . The acoustical driving pressure is taken to be  $P_a(t) = P_a \sin(\omega t)$ , with  $P_a = 1.4 \text{ atm}$  and  $\omega/2\pi = 25 \text{ kHz}$ .

Our numerical procedure is straightforward: we determine the solutions of the RP-equations, and use these to solve Eq. (16) at a given instant in time. The solutions turn out to be very smooth in time and space and we can interpolate quite easily the solutions with large time steps. Subsequently, we can study any property of the bubble.

When we evaluate, as a function of time, the energy content in the bubble, we find that there are three time scales of interest in the gas bubble dynamics: the overall energy of the liquid and the bubble varies on scale of driving frequency, within the collapse window of a few microseconds, as can be seen in Fig. 1a. Note that we present the energy of the liquid per atom in the gas bubble. The solid line is the total energy, the dotted line is the kinetic energy of flow, the dashed line is the internal (potential) energy arising from the work done on the liquid. Both components contribute significantly to the overall energy of the liquid. We see that the potential energy dips during the

slow expansion phase of the bubble motion, and then smoothly rises to a maximum value at which point it declines at a slightly faster rate. During the collapse the kinetic energy of the fluid rises to  $\mathcal{O}(60 \text{ eV})$  per atom in the bubble gas, which energy is rapidly lost to elastic and inelastic processes when the bubble hits the van der Waals hard core. The dynamical time scale of the fluid, defined as the time difference in minimum-maximum-minimum energy evolution, is  $\mathcal{O}(10 \mu\text{s})$ , corresponding to a quarter of the acoustical driving cycle of  $40 \mu\text{s}$ . The interior gas energy varies on the scale of nanosecond, as can be seen in Fig. 1b. In this example about 7% of the energy is transferred from the liquid to the gas. Finally, in Fig. 1c we show a time-resolved view of the energy contents of the interior of the bubble. We see that most of the energy rise occurs within a 100 picosecond time window. The energy of the bubble disappears rather slowly; there is no viscous damping included in the dynamics of the gas.

We now turn our attention to estimate the intensity of the sonoluminescence arising from the atomic collision processes; for this we obtain the collision frequency of all atoms in the bubble:

$$f_N = N\sigma \frac{\rho}{M_G} v_{\text{rel}}. \quad (18)$$

The effective collision cross section is assumed to be geometric and thus  $\sigma \simeq (4\pi/3a^3/N)^{2/3}$ . A measure of relative velocity is obtained from the total energy per atom  $v_{\text{rel}} \simeq \sqrt{2E/m}$ . We can obtain these results for a number of different conditions of driving pressure, ambient pressure, frequency, etc. In Fig. 2 we present the results for  $P_a = 1.4, 1.3, 1.2 \text{ atm}$ , selecting an arbitrary time axis origin so that these results can be shown together. The number of collisions shown is in  $10^{10}/\text{ps}$ , thus during the light flash duration of  $50 \text{ ps}$  we expect about  $10^{12}$ – $10^{13}$  atom-atom collisions to occur in the bubble. We recall that experimentally observed is the emission of up to million photons in the spectral range of visible light during the same period of time (see e.g. legend of figure 1 in Ref.[3].) We also see in Fig. 2 that the number of collisions is changing smoothly, and in a manner corresponding to the emission intensity observed in the experiment [3]. The vertical lines indicate when in time the average energy per atom exceeds 1 eV. The realm of the frequent collisions at 1 eV and above is well within the 500ps time interval of the most extreme density, as is experimentally reported for SBSL [3]. In our opinion these results strongly support the hypothesis that atomic collisions are the source of the short SBSL light flashes [17], since the number of atomic collisions capable to generate visible photons exceed by the comfortable margin of  $10^6$ – $10^7$  the photon yield.

While the onset of SBSL is a gradual process, depending on the magnitude of the driving acoustical pressure field, and could be explained as the onset of frequent high energy atomic collisions, the disappearance of SBSL when  $P_a > 1.4 \text{ atm}$  is quite sudden. We considered the local sound velocity  $c_s(x)$  in the bubble and compare it to the local flow velocity  $v$ , Eq. (3), and have determined that this condition corresponds to the interior flow velocity in the gas bubble slightly exceeding, near to the surface, the local sound velocity. The flow velocity in the bubble, in units of local sound velocity, is shown for several values of driving pressure  $P_a = 1.4, 1.3, 1.2 \text{ atm}$  in Fig. 3. As  $P_a \rightarrow 1.4 \text{ atm}$ , we see in Fig. 3 that the local flows in the bubble are bound to occur with supersonic velocity. For the development of shock waves just this supersonic condition is required. Since in the experiment  $P_a \simeq 1.4 \text{ atm}$  is the upper limit for the SBSL process, we are led to the hypothesis that it is the onset of shock instability in the bubble, which is responsible for the upper limit in  $P_a$  for which SBSL can occur.

## 5. Discussion and conclusions

In summary, we have developed a semi-analytical dynamical model to describe the properties of the interior of the cavitating gas bubble. In our approach we have simplified the complexity of

the hydrodynamic gas flow problem by exploiting in a variational approach the nearly homologous bubble dynamics. Considering that SBSL occurs in an extremely small domain of a large parameter space, our approach is in some aspects more capable to gain physical insights, than is full hydrodynamics. Several approximations were made: we did not address quantitatively in our numerical work the sound fluctuations inside the bubble during its motion. We did not consider here the back-reaction from the dynamics of the gas bubble to the dynamics of the liquid which, while important in principle, does not change the general dynamic behavior of the bubble [7]. Neither did we include the compressibility in the description of the surrounding fluid motion, but our state of the art implementation of the dynamics of the bubble includes in a way proposed in Ref. [21] the dissipative effects such as viscosity of the fluid, and most importantly, acoustic radiation damping [9, 21]. We checked and agree with Ref. [10] that allowing for compressibility of the liquid in the extreme conditions of SBSL further sharpens the characteristic time scale involved, as the denser liquid can more rapidly acoustically dissipate the air bubble energy. We find that even without this effect there is a natural 100-picosecond time scale in argon cavitation in water, arising from the transfer of kinetic flow energy from the liquid to the gas bubble in its expansion phase, followed by inertial collapse of the energized bubble.

We were able to derive the density shapes of the bubble and to evaluate the energy content of the bubble as function of time. We have shown that the bubble energy has a characteristic relaxation time  $\mathcal{O}(1\text{ ns})$ , while the scale  $\mathcal{O}(100\text{ ps})$  describes the rise in energy of the bubble. We have shown in quantitative fashion that it is likely that atomic collisions are the source of the light flashes seen in SBSL. We refrain here from the evaluation of the CIE rates [17], pending further clarification of microscopic mechanisms (specifically the role of noble gases, three body collisions), and also since this task transcends the scope of this research project. Thus while this is not the time and place to explore in detail the light spectrum that can be produced, we note that during the short time interval allowing deep atomic collisions, CIE will produce light pulses of similar temporal length for different wavelengths in the visible range.

The dynamical properties of the RP-model lead us to believe that it is the (inward) shock instability that poses an upper-applied-acoustical-pressure-limit on the SBSL phenomenon. Specifically, when the strength of the driving acoustical pressure reaches the value at which experimentally SBSL phenomenon suddenly disappears [3], our calculations show that the internal bubble dynamics must evolve faster than local sound velocity. This should lead to flow instabilities, which in all likelihood can destruct the bubble. Our results imply that the complex, near-shock-nonlinear dynamics of the bubble interior combined with light emissions in atomic collision processes can provide a suitable framework to explain the SBSL phenomenon.

## Acknowledgment

Work partially supported by: DOE, grant DE-FG03-95ER40937; by NSF, grant INT-9602920; and by PRONEX-41.96.0886.00 – Brazil.

## References

- [1] D.F. Gaitan, L.A. Crum, C.C. Church, and R.A. Roy, “Sonoluminescence and Bubble Dynamics for a Single, Stable Cavitation Bubble” *J. Acoust. Soc. Am.*, **91**, 3166 (1992);  
D.F. Gaitan, L.A. Crum, “Sonoluminescence From Single Bubbles”, *J. Acoust. Soc. Am. Suppl. 1*, **87**, S141 (1990).
- [2] B.P. Barber and S.J. Putterman, “Observation of Synchronous Picosecond Sonoluminescence” *Nature* **352**, 318 (1991);  
B.P. Barber and S.J. Putterman, “Spectrum of Synchronous Picosecond Sonoluminescence”, *Phys.*



- Rev. Lett* **69**, 1182 (1992);  
B.P. Barber, Ph.D. Thesis, “Synchronous Picosecond Sonoluminescence”, Department of Physics, UCLA, Technical Report BB92 (June 1992), unpublished.
- [3] B.P. Barber, R. Hiller, R. Löfstedt, S.J. Putterman, K.R. Weninger, “Defining the Unknowns of Sonoluminescence”, *Physics Reports*, **281**, 65 (1997)
- [4] S. Hilgenfeldt, D. Lohse, M.P. Brenner, “Phase Diagrams for Sonoluminescing Bubbles”, *Phys. Fluids*, **8**, 2808 (1996); [chao-dyn/9608005], and references therein.
- [5] For prior-1980 work on cavitation and theoretical details and references describing the RP model see: E.A. Neppiras, “Acoustic Cavitation” *Physics Reports*, **61**, 159–251 (1980).
- [6] W. Yourgrau and S. Mandelstam, *Variational Principles in Dynamics and Quantum Theory* Dover, New York 1979.
- [7] T. Kodama, H.-Th. Elze, J. Rafelski, and I. Scott, *APH N.S., Heavy Ion Physics* **5**, 343 (1997).
- [8] M.-C. Chu, “The Homologous Contraction of a Sonoluminescing Bubble”, *Phys. Rev. Lett.* **76**, 4632 (1996).
- [9] H.-Th. Elze, T. Kodama and J. Rafelski, “Sound of Sonoluminescence” *Phys. Rev.* **E57**, 4170, (1998).
- [10] B. Gompf, R. Günther, G. Nick, R. Pecha, and W. Eisenmenger, “Resolving Sonoluminescence Pulse Width with Time-Correlated Single Photon Counting ”, *Phys. Rev. Lett.* **79**, 1405 (1997).
- [11] C.C. Wu and P.H. Roberts, “Shock-Wave Propagation in a Sonoluminescing Gas Bubble”, *Phys. Rev. Lett.* **70**, 3424 (1993).
- [12] W. Moss, D.B. Clarke, J.W. White, and D.A. Young, “Hydrodynamic Simulations of Bubble Collapse and Picosecond Sonoluminescence”, *Phys. Fluids*, **6**, 2979 (1994);  
“Sonoluminescence and the Prospects for Table-Top Micro-Thermonuclear Fusion”, *Physics Letters* **A211**, 69 (1996).
- [13] M.-C. Chu and D. Leung, “Effects of Thermal Conduction in Sonoluminescence”, *J. Phys.: Condens. Matter* **9**, 3387 (1997).
- [14] W. Moss, D.B. Clarke, and D.A. Young, “Calculated Pulse Widths and Spectra of a Single Sonoluminescing Bubble”, *Science* **276**, 1398 (1997).
- [15] K. Weninger, S. J. Putterman and B. P. Barber, “Angular correlations in sonoluminescence: Diagnostic for the the sphericity of a collapsing bubble” *Phys. Rev. E* **54**, R2205 (1996).
- [16] B.P. Barber, lecture comments and [2, 3].
- [17] L. Frommhold and A.A. Atchley, “Is Sonoluminescence Collision-Induced Emission?” *Phys. Rev. Lett.* **73**, 2883 (1994).
- [18] R.A. Hiller, S.J. Putterman, and K. R. Weninger, “Time-resolved Spectra of Sonoluminescence”, *Phys. Rev. Lett.* **80**, 1090 (1998).
- [19] A. Prosperetti, “A New Mechanism for Sonoluminescence”, *J. Acoust. Soc. Am.* **101**, 2003 (1997).
- [20] K. R. Weninger, B. P. Barber, and S.J. Putterman “Pulsed Mie Scattering Measurements of the Collapse of a Sonoluminescing Bubble”, *Phys. Rev. Lett.* **78**, 1799 (1997).
- [21] R. Löfstedt, B.P. Barber, and S.J. Putterman, “Toward a Hydrodynamic Theory of Sonoluminescence”, *Phys. Fluids* **A5**, 2911 (1993).

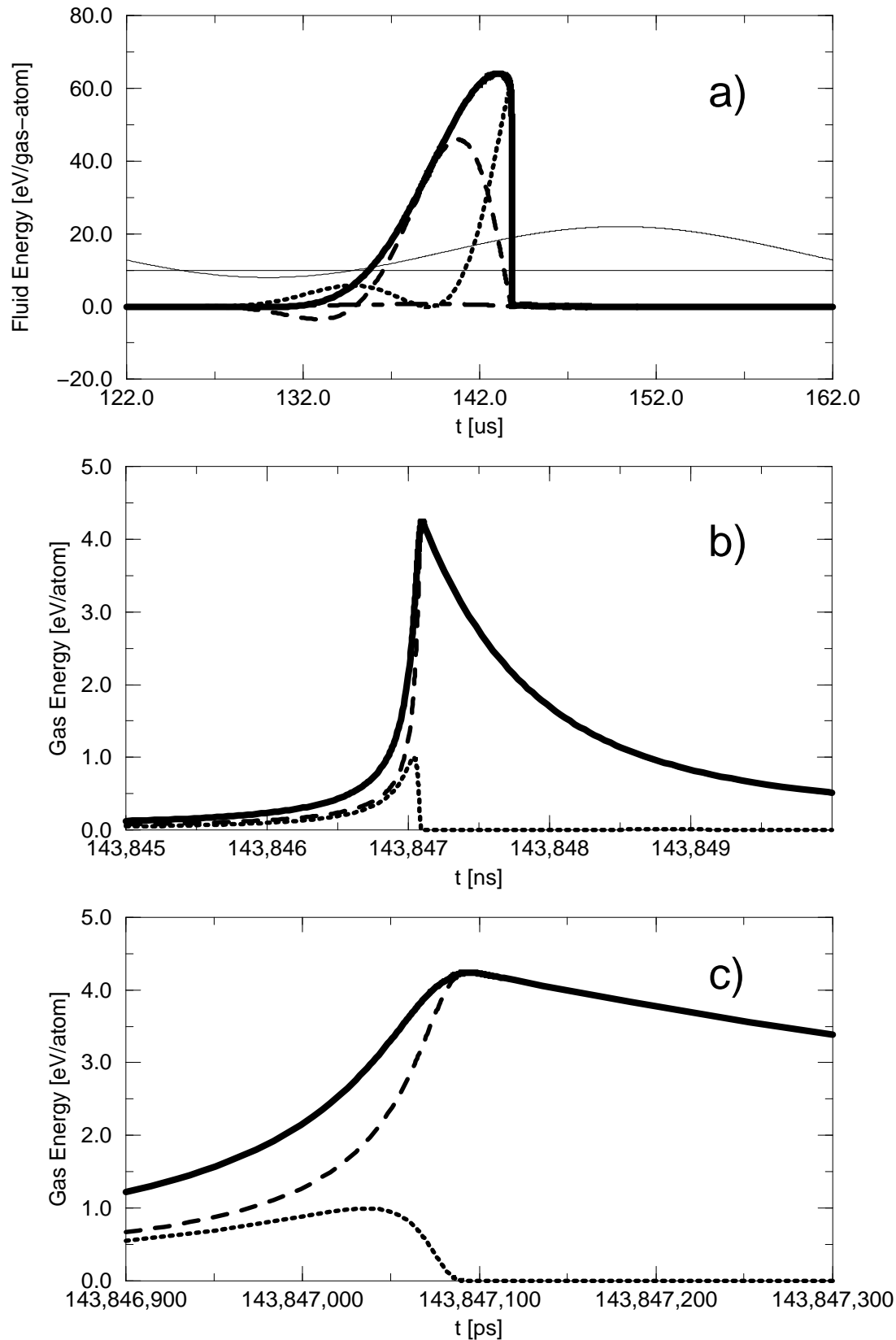


Figure 1: Argon bubble with  $10^{10}$  atoms in water. Evolution of gas bubble energy: dotted line is the kinetic energy, dashed line is the potential energy, and solid line is the total energy. The thin solid line over arbitrary scale shows the sum of ambient pressure, 1 atm, and driving acoustical pressure ( $\omega = 25$  kHz), amplitude at bubble surface 1.4 atm: a) The energy in the fluid in eV per atom in the bubble; b) The energy in the bubble over nanosecond time scale; c) The fine resolution in time of the bubble energy during most extreme collapse.

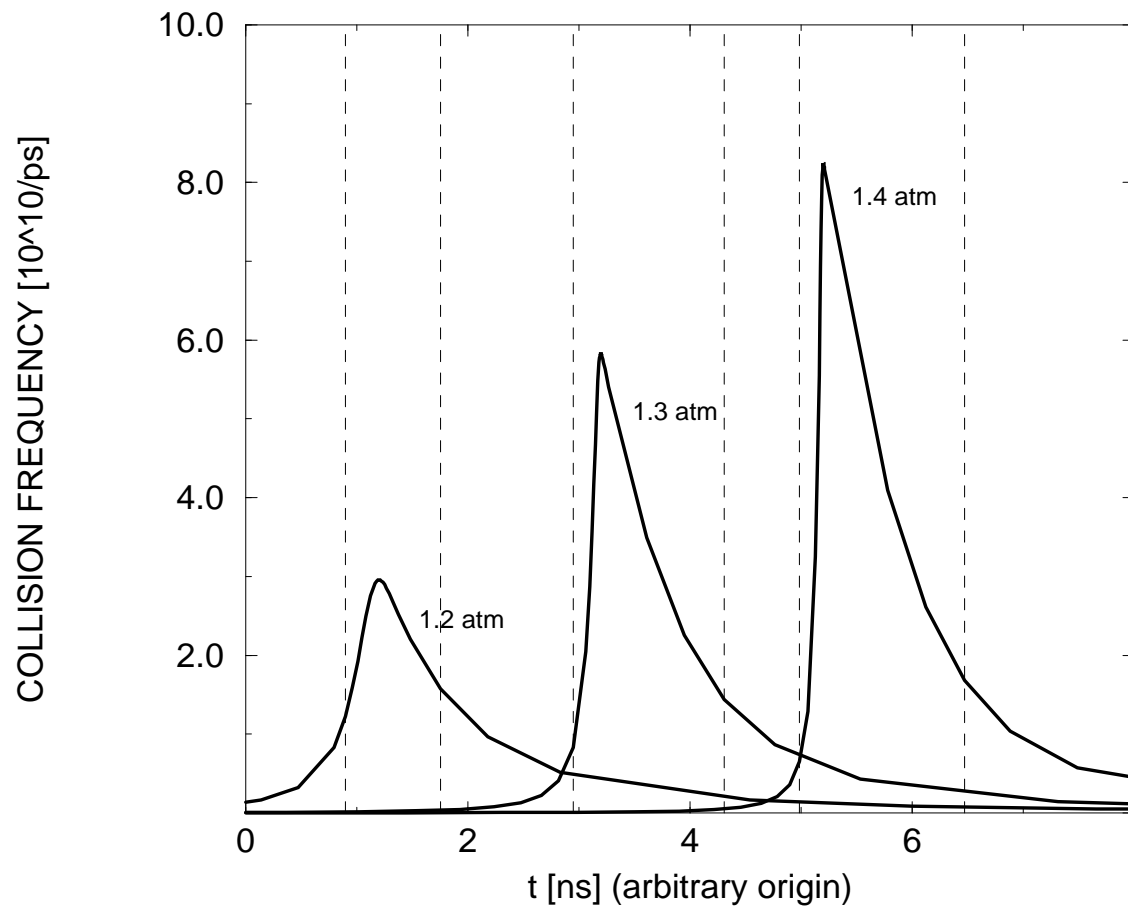


Figure 2: Number of atom-atom collisions (times  $10^{10}$ ) per picosecond in the bubble as function of time for three values of driving acoustical amplitude,  $P_a = 1.2, 1.3, 1.4$  atm. Dashed vertical lines delimit range for 1 eV energy per atom in the bubble.

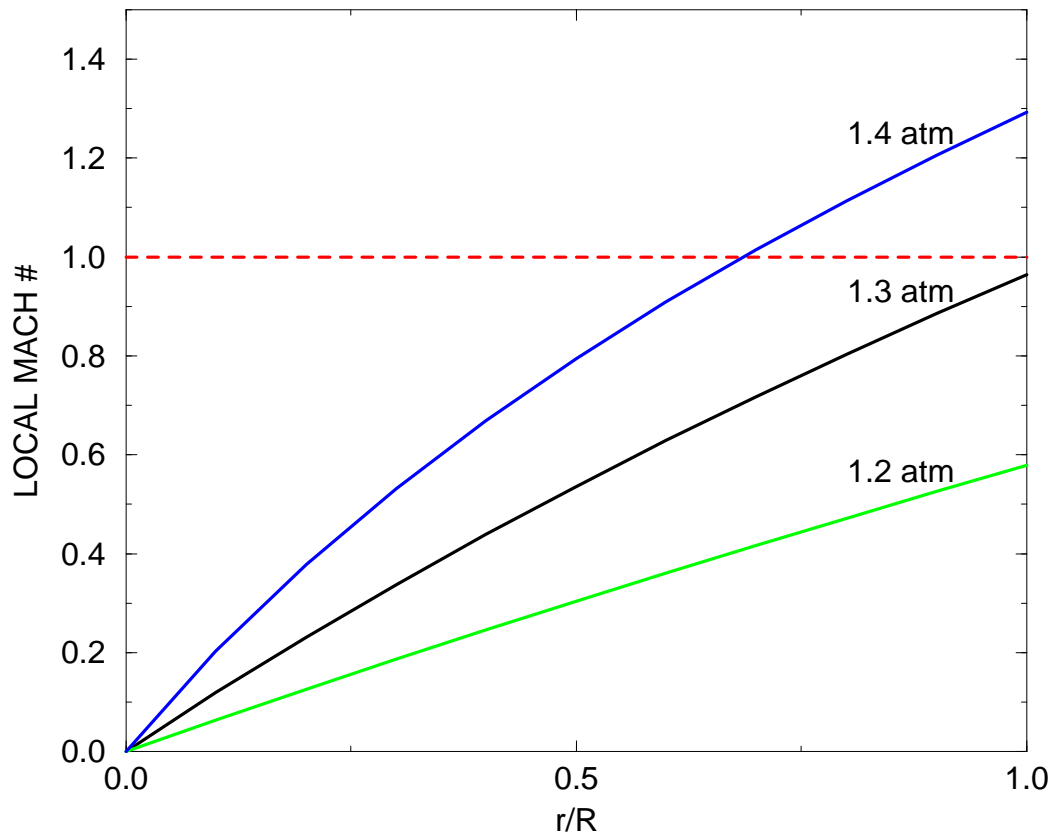


Figure 3: Local flow velocity in units of the local sound velocity (termed Mach #), as function of the scaled radial coordinate of the bubble,  $r/R$ . Dashed line: Mach # = 1.0. Results for driving pressure  $P_a = 1.4, 1.3, 1.2$  atm are shown (top to bottom). Event time chosen to maximize the local Mach # at the bubble surface.